Title: SARS-CoV-2 variant natural evolution in K18-ACE2 mice increases virulence and produces treatment resistance-linked variant alleles.

Authors: Julian Daniel Sunday Willett[1,2,3], Annie Gravel[4], Isabelle Dubuc[4], Leslie Gudimard[4], Paul Fortin[4,5,6], Ju-Ling Liu[2,8], Jose Avila Cervantes[9], Jose Hector Galvez[7], Melissa Zwaig[2,8], Anne-Marie Roy[2,8], Sally Lee[2,8], Shu-Huang Chen[2,8],Jiannis Ragoussis[2,8]*, Louis Flamand[4,10]*

Affiliations:

1. Quantitative Life Sciences Ph.D. Program, McGill University, Montreal, QC, Canada
2. McGill University Genome Centre, Montreal, QC, Canada
3. Lady Davis Institute, Jewish General Hospital, Montreal, QC, Canada
4. Axe maladies infectieuses et immunitaires, Centre de Recherche du Centre Hospitalier Universitaire de Québec- Université Laval, Canada
5. Centre de Recherche ARThrite-Arthrite, Recherche et Traitements, Université Laval, Québec, QC, Canada.
6. Division of Rheumatology, Department of Medicine, CHU de Québec-Université Laval, Québec, QC, Canada
7. Canadian Centre for Computational Genomics, McGill University, Montreal, QC, Canada
8. Department of Human Genetics, McGill University, Montreal, QC, Canada
9. Advanced Genomic Technologies Laboratory, McGill Genome Centre, McGill University, Montreal, QC, Canada.
10. Département de microbiologie-infectiologie et d'immunologie, Université Laval, QC, Canada.

*Co-corresponding authors

Abstract:

The continuing COVID-19 pandemic is partially due to viral evolution reducing vaccine and treatment efficacy. Others have observed serial infections in mice with reference SARS-CoV-2 lineage IME-BJ05 produce adapted strains with significantly greater infectivity and mortality. We investigated the impact of long-term B.1.351 (Beta) and B.1.617.2 (Delta) lineage viral evolution in K18-ACE2 mice, which express human ACE2 receptor. We infected mice with these unmodified variants in a BSL-3 laboratory and studied viral evolution across 20 passages without selective pressure, sequencing virus at key points. Our IRB determined the research was not gain-of-function. We observed variant alleles with documented contributions towards evading vaccine-induced immunity arise *de-novo*, including Omicron-characteristic mutation S371F. Passage 20 (P20) viruses were more virulent, and P20 Delta was significantly more resistant to antibody neutralization. These developments occurred rapidly, emulating pandemic progression in non-immune mammals. Our model could be rapidly adapted to include selective pressures to study the evolution of viruses resistant to antivirals or vaccine-induced immunity.

Keywords: SARS-CoV-2, COVID-19, pandemic modelling, treatment resistance, viral evolution.

41 ## Introduction:

42 Part of the difficulty in responding to the COVID-19 pandemic has been predicting viral evolution
43 and its impact on clinically relevant traits, such as infectivity, treatment resistance, and disease
44 severity[1]. The basic biology of the severe acute respiratory syndrome Coronavirus 2 (SARS-
45 CoV-2), the virus that causes COVID-19, is well understood. However, knowledge of SARS-
46 CoV-2 evolution is limited. Many RNA viruses, such as SARS-CoV-2, exist as quasi-species
47 meaning that within a given viral population, a multitude of alleles (major and minor) are
48 present. These alleles give plasticity to the viral population allowing for rapid
49 adaptation/selection to a variety of circumstances[2]. Viral evolution is also complex and affected
50 by several factors, including host genetic background[3], host immune status[4], the organs
51 targeted by the virus[5], and a population's collective immunity[6]. As a result, it has been difficult to
52 predict the emergence of new variants with altered virulence.

53 Several variants of concern (VOC) have emerged, each with mutations providing dissemination
54 advantages[1]. For example, the SARS-CoV-2 alpha variant (B.1.1.7) gained a growth advantage
55 and rapidly spread globally due to the spike protein N501Y mutation that enhances affinity for
56 the cellular entry receptor, angiotensin-converting enzyme 2 (ACE2)[7]. Other VOC, such as the
57 Delta (B.1.617.2) variant, gained advantages with additional substitutions in spike, including
58 L452R[8], T478K[9], and P681R[10] that affect viral transmissibility and antibody neutralization for
59 naturally or artificially vaccinated individuals[11]. To better predict changes in SARS-CoV-2 and
60 reduce the impact of a future pandemic, time effective models must be defined for studying viral
61 changes over successive generations.

62 In 2020, Gu *et al.* studied short-term viral evolution by infecting aged mice with the SARS-CoV-2
63 reference strain (IME-BJ05) and collecting lung tissue at set timepoints following infection, using
64 this isolate to infect successive generations of mice[12]. While wild-type mice are thought less

65 susceptible to the virus as mouse Ace2 is not used by SARS-CoV-2 as its receptor, Gu *et al.*
66 demonstrated that serial passaging of lung homogenate across mice produced a mouse-
67 adapted strain (MASCp6) that causes pulmonary symptoms, matching adaptations observed by
68 others who previously applied the technique to influenza[12,13]. After six passages, they found
69 several clinically relevant genetic changes, including de-novo appearance of A23063T that
70 changes spike to N501Y[12]. This mutation is associated with enhanced viral infection and
71 transmission[7]. Subsequently, the group passaged the MASCp6 isolate an additional 30 times
72 and characterized the MASCp36 isolate[14]. MASCp36 contained several mutations (i.e. K417N,
73 Q493H and N501Y mutations) in spike conferring greater Ace2 receptor binding affinity,
74 increased infectivity and greater virulence[14]. Others replicated this study using the same viral
75 variant, observing similar development of clinically relevant variant alleles[15].

76 Since these studies, new lineages arisen, with the present being Omicron, negatively impacting
77 treatment efficacy[1]. Others have studied viral dynamics using recent lineages in serial passages
78 in cells, observing similar development of directional selection and clinically concerning
79 mutations[16,17]. Given the pandemic's prolonged nature, understanding longitudinal viral changes
80 in a mammalian host is pressing. We adapted Gu *et al.*'s approach to evaluate how viral
81 lineages more closely related to the present lineages, B.1.351 (Beta) and B.1.617.2 (Delta),
82 changed over twenty passages[12] in transgenic mice with human ACE2 receptors, instead of
83 murine. Given clinically relevant mutations arising in Gu *et al.*'s studies[12,14], we sought to
84 determine if impactful variant alleles would develop in more recent viral variants. We report on
85 the *de novo* appearance and persistence of variant alleles associated with treatment resistance
86 with serially passaged virus demonstrating increased virulence and antibody resistance.

87

88

Results:

Variant allele frequency of alleles across passages. To ensure effective comparisons between key viral passages, we downsampled sequencing reads for each period of the study (**Figure 1**). The minimum number of reads per sample in the first part of the study across passage 0 (P0) and P10 was 8,812,604. The minimum number of reads per sample in the second part of the study across P13, P17, and P20 was 34,253,784. In Beta lineage, there was a significantly lower variant allele frequency (VAF) in P17 and P20 versus other passages (adjusted p-value < 0.05), with a significant difference in Delta comparing P10 and P20 (**Figure 2a-b**). As there was no significant change in allele depth across the study, these VAF differences could be due to growing allelic diversity. Such significant changes, less consistent with random allelic drift, could align with suggested mechanisms of within-host evolution of the variant allele pool, per Tonkin-Hill *et al.*[18]. Sample contamination is less likely as there was no significant difference in VAF or variant allele depth between samples for either viral lineage (**Figure 2c-d**).

Gene involvement and variant allele functional consequence severity did not significantly vary across passages. To evaluate for large-scale variant allele shifts across the study, we used chi-squared tests, adjusted for multiple-testing, to compare the net proportion change in variant allele subcategories by passage. There was no statistically significant change in the proportion of variant alleles involving a specific gene or severity of variant allele predicted functional consequence across the study (adjusted p-value > 0.05) (**Figure 3**), suggesting that the overall allele population did not significantly change in our model without experimental selective pressures [6].

Development of variant alleles associated with clinically relevant traits. To study viral evolution in our model at the single variant allele level, we identified those variant alleles that changed in frequency across passages, including those that arose *de novo* and disappeared, and annotated them for clinically relevant traits. We observed 82 unique variant alleles across our

114 study. There were 41 whose VAF changed with 32 having clinically-relevant annotations,
115 including interactions with human proteins, mutations that may confer drug resistance, variant
116 alleles associated with the Omicron lineage, mutations associated with antibody escape, and
117 mutations at vaccine targets (**Table 1, Supplemental Table 1**) [19,20]. A notable novel variant
118 included C22674T, or Spike S371F, that arose *de-novo* in two animals in P20 for Beta virus and
119 two animals in P13 for Delta virus (**Figure 4**). The allele is associated with protein interactions,
120 antibody escape, affects a vaccine target, and is an Omicron-specific mutation (**Table 1**) [20,21].
121 We thus observed an Omicron specific mutation in a study not involving Omicron viral lineages.
122 Several other variants changing in frequency also conferred possible drug resistance and
123 targeted the vaccine site (**Table 1**) [20].

124 Most alleles in the P0 Beta isolate, passaged several times *in vitro* in Vero cells, encoded a
125 Spike protein with a tryptophan (W) at position 682 (C23606T), destroying the furin cleavage
126 site (**Table 1**). We observed a rapid selection of viruses having the reference allele encoding an
127 arginine (R) at position 682 and functional furin site in all animals infected with Beta variant
128 starting in P10 (**Table 1**). This suggests that the furin site provides a growth advantage under *in*
129 *vivo* conditions and supports a previous report indicating the Spike furin site being important for
130 SARS-CoV-2 virulence in K18-ACE2 mice [22].

131 *Later passage viruses cause greater weight loss and viral loads and demonstrate reduced*
132 *neutralization by immune sera*. To study our model's viral evolutionary impact on the organism
133 level, we compared clinical scores of mice infected with early and late passaged virus. Unlike
134 Gu *et al*.'s study that required adaptation of SARS-CoV-2 to a murine Ace2 receptor for
135 infectivity, our study made use of transgenic mice expressing the human ACE2 receptor [12]. We
136 determined whether repeated passaging of SARS-CoV-2 in K18-ACE2 mice affected virulence
137 by infecting animals with P0 and P20 viruses with clinical scores and viral loads determined. On
138 day 3 post-infection, no differences in viral load were noted between Beta P0 and Beta P20

139 viruses with mice infected with P20 Delta virus having a significant increase (6.3x) in lung viral
140 loads (**Figure 5A**). Both P20 Beta and P20 Delta viruses caused more rapid and greater weight
141 loss than P0 viruses (**Figures 5B-C**) with similar survival curves (data not shown).

142 We then assessed whether repeated passages in K18-ACE2 mice would result in viruses
143 capable of infecting non transgenic mice. C57BL6 mice were infected intranasally with P0 and
144 P20 viruses and lung infectious viral loads determined 3 days later. Both P0 and P20 Beta
145 viruses successfully replicated in mouse lungs with both viruses producing similar viral loads
146 (**Supplementary Figure 2**). None of the P0 or the P20 Delta viruses generated viral loads in
147 lungs of B6 mice (**Supplementary Figure 2**).

148 Our results indicate that Delta P20 viruses generate a greater viral load that P0. To determine if
149 this was related to growth kinetic differences between P0 and P20 viruses, we performed *in vitro*
150 growth curve analysis. We observed two independently evolved P20 Delta viruses replicating
151 more efficiently after 24 h versus P0, yielding 4-5X more infectious virus after 24h of infection
152 (**Figure 6**). This difference in viral titers was no longer observed after 48 h (**Figure 6**).

153 We next determined the ability of sera from vaccinated subjects to neutralize passaged viruses,
154 comparing it to parental P0 viruses. Consistent with previous reports, sera from vaccinated
155 subjects had varied neutralizing potential depending on the variant, with neutralization titers
156 being greatest against the original Wuhan-like strain and lowest for the Beta isolate (**Figure 7A**)
157 [23,24]. The same sera were analyzed for their ability to neutralize P20 viruses. P20 Beta was
158 neutralized equally (13 out of 24) or more efficiently (8 of 24) that the P0 virus (**Figure 7B**). In
159 contrast, P20 Delta virus was significantly less sensitive to antibody neutralization by vaccinated
160 subject sera than P0 ($p < 0.0002$) where 15 of 24 sera showed decreased neutralizing potential
161 toward the P20 Delta virus relative to P0 (**Figure 7C**).

162

163 **Discussion**:

164 In this study, we serially infected mice with Beta or Delta lineage virus for twenty passages
165 without experimental selective pressures. The evolved viruses developed and maintained
166 variant alleles associated with treatment resistance and later lineages like Omicron (**Figure 4,**
167 **Table 1**), were more virulent (**Figure 5**), grew faster and to higher levels (Delta) (**Figure 6**) and
168 were less sensitive to antibody neutralization (Delta) (**Figure 7**), demonstrating immune escape
169 potential. These developments occurred within roughly two months, illustrating the model's
170 potential in rapidly emulating pandemic progression that could facilitate treatment/vaccine
171 development less sensitive to viral evolution. The model can readily be adapted to mimic viral
172 adaptation in the context of immune or anti-viral selection pressures, affording rapid results in a
173 system often seen in real world conditions.

174 Our model lacked experimental selective pressures, mimicking the evolution of SARS-CoV-2 in
175 a naïve population. Using K18-ACE2 transgenic mice eliminated the selective pressure of
176 adapting virus to the murine Ace2 receptor. The Beta P0 virus harbored the N501Y mutation
177 previously reported to enable adaptation of reference SARS-CoV-2 in non transgenic mice [12].
178 This mutation was maintained throughout passages, suggesting that this virus can infect cells
179 through the murine Ace2 receptor as well (**Figure 4**). Our data supports this, as non transgenic
180 C57BL6 mice were equally susceptible to infection by Beta P0 and P20 viruses. This capacity of
181 Beta to use human and murine receptors might explain, at least in part, the greater virulence of
182 the Beta isolate in ACE2 transgenic mice relative to other viral isolates, such as Wuhan and
183 Delta lacking the N501Y mutation in transgenic mouse studies [25].

184 The Delta P0 virus lacked the N501Y mutation and never acquired it following repeated
185 passages in ACE2 transgenic mice. This highlights that when lacking selective pressure, such
186 as neutralizing antibodies, the appearance of N501Y is not favored (**Figure 4**). Acquisition of

187 N501Y in the human population was first reported almost a year after the initial report of the
188 SARS-CoV-2 epidemic, suggesting that this mutation arose during the development of herd
189 immunity [26].

190 Of the 41 variant alleles that arose *de-novo* or changed in frequency during the study, several
191 are of clinical interest (**Figure 4, Table 1**). A4981G, which arose *de-novo* and persisted in Beta
192 lineage virus in P17 (**Figure 4**), was predicted to possibly confer drug resistance to papain-like
193 protease inhibitors [27], such as ritonavir used clinically in combination with nirmatrelvir that
194 protects patients against severe COVID-19 [28,29]. C22674T, or spike S371F, which arose *de-*
195 *novo* and persisted in two animals in P20 for Beta and P13 for Delta virus (**Figure 4**), represents
196 an Omicron-specific mutation arising in a study that did not use Omicron. This last mutation has
197 been previously reported to facilitate antibody escape (**Table 1**) [21]. Considering that the
198 mutation S371F is reported to bear a significant fitness cost [30], this might explain why isolated
199 S371L/F mutations are not viable or have not yet been detected in isolation. We would argue
200 that mutations of residues E484 present in Delta and K417/E484/N501 present in Beta Spike
201 proteins, also found together with the S371F mutation in Omicron BA.2, represent such
202 compensatory mutations. G23593T, or spike Q677H, which disappeared from Beta virus
203 samples after P0, has been determined to enhance treatment resistance and increase viral
204 infectivity [31]. The reversion of Spike amino acid 677 to Q after passage in mice could explain the
205 increased neutralization activity for some of the sera against Beta P20 relative to P0 (**Figure 7**).
206 Variants that could impair treatment efficacy appeared and disappeared in this study,
207 showcasing the model's potential in evaluating diverse variants.

208 This study has limitations. Here we used the K18-ACE2 transgenic mice but the mechanisms of
209 new viral variants arising in humans could significantly differ. This is relevant as host factors are
210 believed to contribute to viral variant allele diversity [32]. Our model lacked experimental selective
211 pressures, while the COVID-19 pandemic has been accompanied by contact limitations and

212 vaccines with the dominant SARS-CoV-2 evolutionary mechanism believed to be natural
213 selection [6]. Development or dominance of new variants likely varies with these pressures,
214 necessitating reproducing this model with them. However, a baseline comparison model is
215 required to get the most from these supplemental models, hence the relevance of our model.
216 We studied Beta and Delta lineage virus, which are no longer dominant. Patterns of genetic
217 changes observed in these lineages could vary from Omicron. There was no statistical change
218 in the variant allele population's involvement of specific genes or predicted functional
219 consequence when comparing Beta and Delta lineages across passages, which is reassuring
220 for generalizability. However, virulence significantly increased across the study, despite this lack
221 of population-level changes (**Figure 5**). This could suggest greater value in studying changes in
222 single variant alleles over allele populations, as done in this study, as they are associated with
223 fitness-related traits and can capture evolutionary changes of more subtle mechanisms, such as
224 increasing virus adaptation for cellular infection. Single or combinations of variant allele changes
225 could explain the change in virulence and antibody neutralization observed in this study (**Figure**
226 **4**).

227

228 **Conclusions**:

229 The model presented rapidly emulated pandemic progression in a naïve population, with virus
230 accumulating variant alleles that could limit therapies for severe disease, becoming more
231 virulent, and ultimately becoming treatment resistant in mice harboring human ACE2 receptor.
232 These results support that serial viral passaging in mice is a useful method to rapidly study viral
233 evolution enabling development of targeted anti-viral therapies.

234

235

236 **Methods:**

237 ***Viruses.*** SARS-CoV-2 Wuhan-like strain (LSPQ, B1 lineage) was obtained from the Laboratoire
238 de Santé Publique du Québec ([LSPQ] Sainte-Anne-de-Bellevue, QC, Canada). SARS-CoV-2
239 Beta strain was obtained from BEI resources and SARS-CoV-2 Delta strain from the BC
240 Centers for Disease Control. Unmodified SARS-CoV-2 strains were propagated on Vero cells
241 (American Type Culture Collection, Manassas, Virginia, USA).

242 ***Determination of the viral titer*.** Vero cells were plated in a 96-well plate ($2x10^4$/well) and
243 infected with 200µl of serial dilution of the viral preparation or lung homogenate in the M199
244 media supplemented with 10mM HEPES pH 7.2, 1mM of sodium pyruvate, 2.5g/L of glucose,
245 5µg/mL *Plasmocin*® and 2% FBS. Three days post-infection plates were analyzed using a
246 EVOS M5000 microscope (ThermoFisher Scientific, Waltham, MA, USA) and the viral titer was
247 determined using the Karber method [33].

248 ***Mouse models***. B6.Cg-Tg(K18-hACE2)2Prlmn/J (stock#3034860) and B6 mice were
249 purchased from the Jackson Laboratories (Bar Harbor, ME). All mouse studies were conducted
250 in a BSL-3 laboratory. One K18-ACE2 mouse was intranasally infected with either B.1.351
251 (Beta) or B.1.617.2 (Delta) SARS-CoV-2 lineages. Following 3-4 days, the animals were
252 sacrificed and lung homogenate collected. The homogenate was used to intranasally infect
253 sequential animals, defined as passage. This was repeated for 10 passages. After passage 10
254 (P10), virus in lung homogenate was sequenced. K18-ACE2 mice were then intranasally
255 infected with Beta P10 or Delta P10 with viruses passaged in three mice at a time for an
256 additional 10 times (total of 20 passages) with virus in lung homogenate sequenced following
257 passages 13, 17, and 20 (**Figure 1**). Viral stocks were then made from lung homogenates of
258 Beta and Delta P20 viruses. K18-ACE2 mice were infected intranasally with 500 $TCID_{50}$ of P0 or
259 P20 viruses. Lung viral loads were determined on day 3 post-infection with weight loss and
260 survival monitored daily for up to 9 days.

261 ***Infectivity of P0 and P20 viruses to non-transgenic mice***. C57BL6 mice were infected
262 intranasally with 3000 $TCID_{50}$ of P0 and P20 Beta and Delta viruses. Three days later, mice
263 were euthanized, and lungs collected for viral load (titer) determination.

264 ***RNA extraction***: Up to 30 mg of lung tissue were used for RNA extraction using the Bead Mill
265 Tissue RNA Purification Kit and the Bead Mill Homogenizer, following manufacturer's
266 instructions.

267 ***Viral sequencing***. RNA extracts were processed for reverse transcription (step a) and targeted
268 SARS-CoV-2 amplification using the ARTIC V3 or V4.1 primer scheme (https://github.com/artic-
269 network/primer-schemes/tree/master/nCoV-2019) (step b). Samples were purified (step b) and
270 Nextera DNA Flex library preparation (step c) was performed for Illumina PE150 paired-end
271 amplicon sequencing on a NovaSeq or MiSeq instrument at the McGill Genome Centre using
272 best practices. Each sample was sequenced twice on different days to obtain a target of
273 minimum 10 million reads per sample. The detailed protocols can be accessed with the
274 following links.

275 Step a: dx.doi.org/10.17504/protocols.io.bjgekjte.

276 Step b: dx.doi.org/10.17504/protocols.io.ewov18e4ygr2/v2.

277 Step c: dx.doi.org/10.17504/protocols.io.bjgnkjve.

278

279 ***Genome data processing*.** Following sequencing, the reads from each sample were used to
280 call variants using Freebayes v1.3.6 [34] and the results were saved as a VCF file which was used
281 to compare genomic variation across passages. Others have called variants with other tools
282 such as DeepSNV [18] and VarScan [35]. DeepSNV was not used as it only investigates SNVs [36],
283 when indels have been found to confer selective advantages [37]. Freebayes has been observed

284 to perform slightly superiorly than VarScan when calling variants in wastewater samples [38] and
285 in internal benchmarking (data not shown). The process is described briefly as follows: first, the
286 raw reads from each sample were aligned with BWA MEM v0.7.17 [39] to the reference strain
287 genome sequence (NC_045512.2). The resulting alignments were sorted with duplicate reads
288 flagged. The minimum number of aligned reads for each was logged, and each sample was
289 again aligned and processed, then randomly down sampled to match this minimum number of
290 reads. All variants with a quality of less than 20 or a depth below 10 were removed from the
291 analysis. Any variant alleles that overlapped with ARTIC sequencing primers were also
292 removed. Merged VCF files, representing the combination of reads across two sequencing
293 batches for each sample, were used for the paper's main results.

294 ***Variant annotation***. Every variant allele was inputted into COVID-19 Ensembl variant effect
295 predictor (VEP) (https://covid-19.ensembl.org/index.html) to determine functional consequences
296 and the involved gene and amino acid change [40]. Variants whose VAF changed at least once
297 across passages during the study were logged and input to the UCSC Genome Browser
298 (https://genome.ucsc.edu/), checking for annotations of antibody escape, CD8 escape, vaccine
299 targets, drug resistance, or variants of concern [20].

300 ***Antibody neutralization studies***. Sera from twenty-four healthy vaccinated (3x) individuals
301 were analyzed for neutralizing activity against Wuhan-like, and Beta and Delta P0 and P20
302 viruses. Serially diluted sera (in quadruplicate) were incubated with 100 $TCID_{50}$ of virus for 1 h
303 at 37˚C before addition to Vero E6 cells. Three days later, the 96-well plates were observed
304 using an inverted microscope for signs of infection. Neutralization titers were determined and
305 defined as the highest serum dilution preventing infection.

306 ***Ethics***. The study was conducted in accordance with the Declaration of Helsinki, and mouse
307 protocols were approved by the Comité de protection des animaux de l'Université Laval. Our
308 IRB determined that our work did not constitute gain-of-function research as virus was

309 unmodified and represented circulating variants with the study conducted without experimental
310 selective pressures. Sera obtained from humans were procured following ERB approval (ERB
311 #2022-6204).

312 ***Statistics and reproducibility***. All statistical analyses were conducted using R/4.2.1. All
313 statistical comparisons between passages were corrected for multiple testing using a Benjamini-
314 Hochberg p-value adjustment. Reproducibility is described in each method.

315 ***Source code***. All code used in this study, from sample processing to data analysis, are publicly
316 available on Github at the following link:
317 https://github.com/juliandwillett/SARS_CoV_2_Serial_Passaging_Study.

318 ***Data availability***. VCF files used to complete computational analyses are available by
319 reasonable request.

320

321 **Declarations:**

322 ***Competing interest***.

323 All authors declare no competing interests.

324 ***Authors contributions***. Julian Daniel Sunday Willett conceived of the computational analyses
325 needed for this study, completed all computational analysis of viral sequencing data, and wrote
326 the majority of the manuscript. Louis Flamand and Jiannis Ragoussis conceived of the study.
327 Louis Flamand contributed to manuscript revisions, wrote sections relevant to animal models
328 and antibody neutralization studies and performed analysis of results. Jiannis Ragoussis
329 supervised sequencing data generation and analysis. Isabelle Dubuc and Leslie Gudimard
330 performed all works involving live SARS-CoV-2 viruses. Annie Gravel participated in the
331 sequence analysis and methodological design of experiments. Paul Fortin and Ines Colmegna

provided key reagents. Jose Hector Galvez contributed bioinformatics analysis review and manuscript revisions. Ju-Ling Liu, Jose Avila Cervantes, Anne-Marie Roy, Sally Lee and Shu-Huang Chen supported the SARS-CoV-2 viral sequencing.

Acknowledgments.

This research was enabled in part by support provided by Calcul Québec (calculquebec.ca) and the Digital Research Alliance of Canada (alliancecan.ca). This study was supported by the Canadian Institutes for Health Research (CIHR 476575) to JDSW, and an operating grant to the Coronavirus Variants Rapid Response Network (CoVaRR-Net) to LF and IR and CIHR grant (GA1-117694) to LF. The funding body had no role in the design of the study or collection, analysis, interpretation, or reporting of the data. We thank Ines Colmegna for providing vaccinated patient sera. We thank Silvia Vidal for her guidance regarding SARS-CoV-2 evolutionary mechanisms. ChatGPT was used to decrease the word count in the abstract with output carefully examined for representing our results.

345 **Figures**:

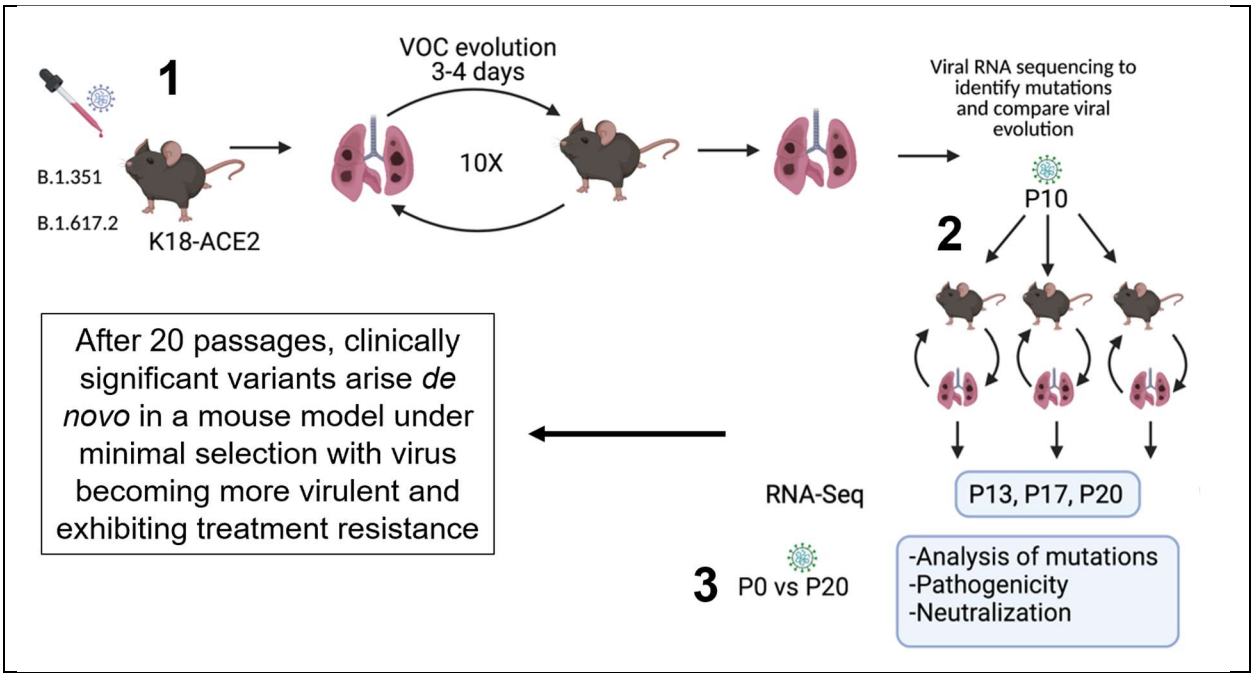

346 **Figure 1**. **Study design**. First, SARS-CoV-2 ACE2-adapted mice were inoculated with either
347 B.1.351 (Beta) or B.1.617.2 (Delta) virus and left for three days for virus to proliferate. They
348 were then sacrificed with the lung homogenate used to infect another mouse. This was repeated
349 for ten passages. Second, P10 virus for each lineage was used to infect three additional mice
350 and the process was repeated for an additional ten passages. Third, P0 and P20 virus for each
351 lineage was used to infect additional mice to compare weight loss and survival between early
352 and late passage virus, and test non-adapted mouse susceptibility to the virus. Antibody
353 neutralization of virus was also compared.

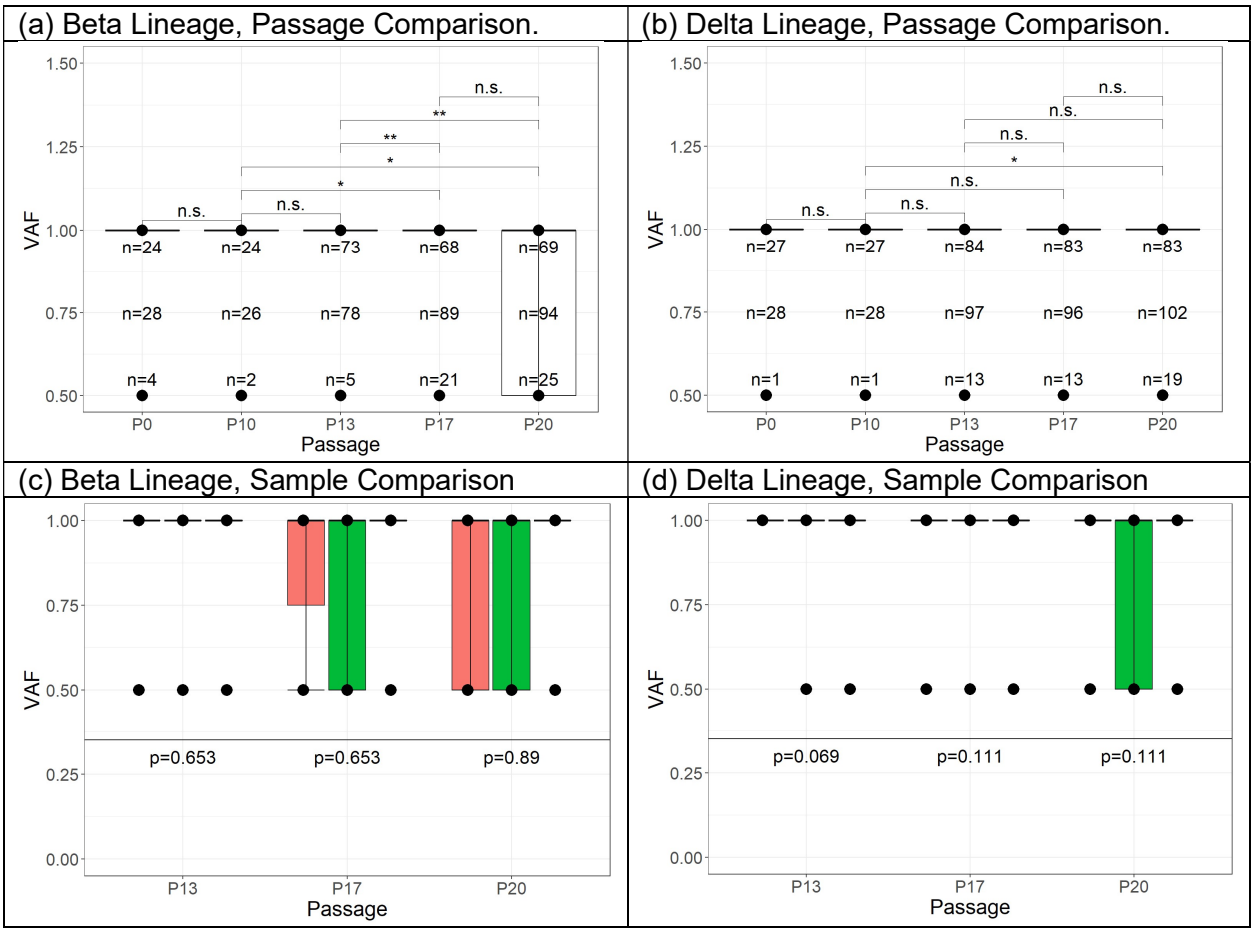

Figure 2. Boxplots of variant allele frequency by (a-b) passage and (c-d) sample. Each N refers to the number of variant alleles for each MAF and in total against the NC_045512.2 reference sequence. Single samples were sequenced for P0 and P10 with three samples from P13, P17, and P20. Box fill in (c-d) signifies sample number. For significance, n.s.: adjusted p-value > 0.05, *: adjusted p-value > 0.01, **: adjusted p-value ≤ 0.01.

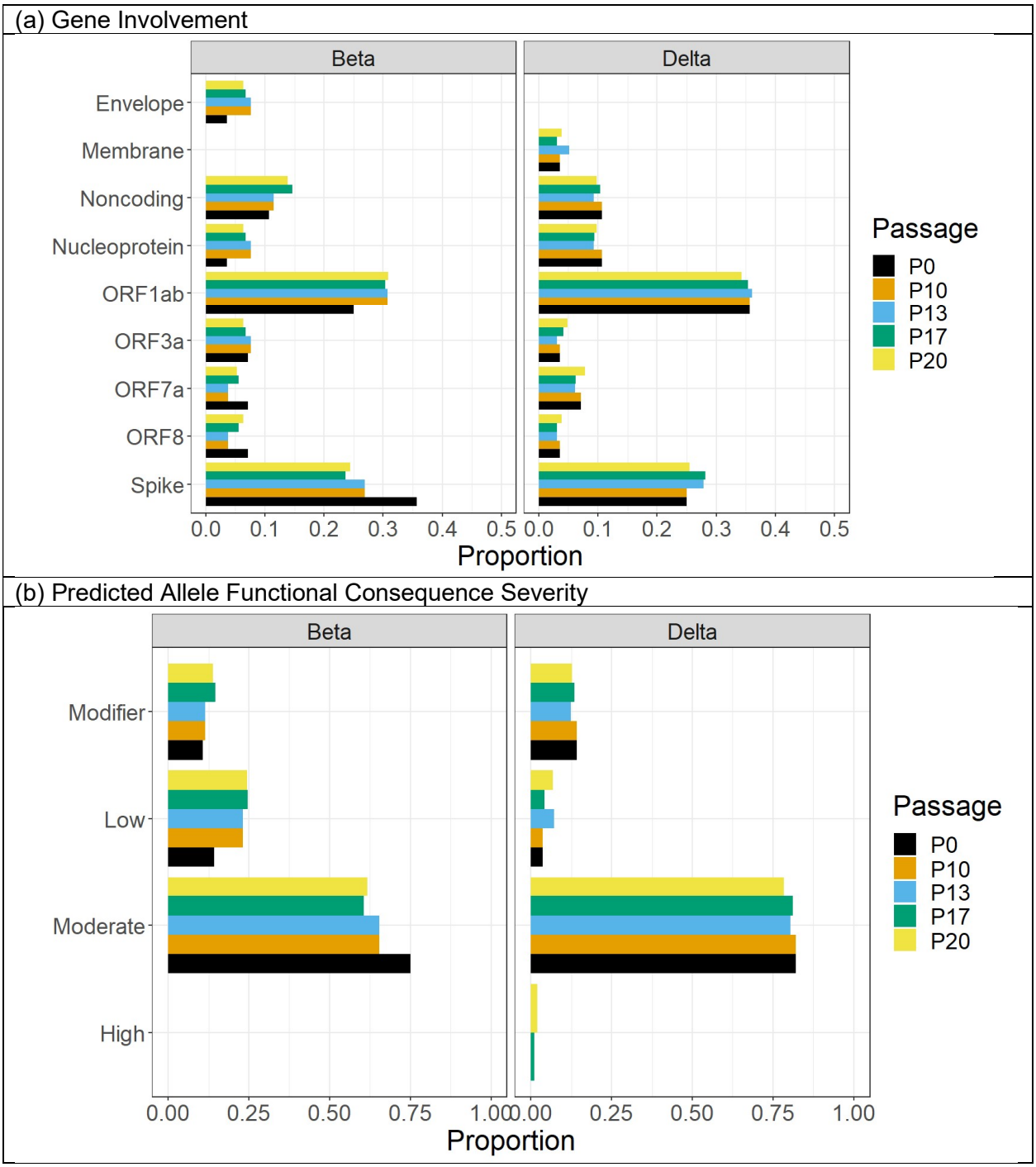

Figure 3. Gene involvement and predicted variant allele functional consequence severity (VEP) in variant allele population did not significantly change (adjusted p-value > 0.05) with passage.

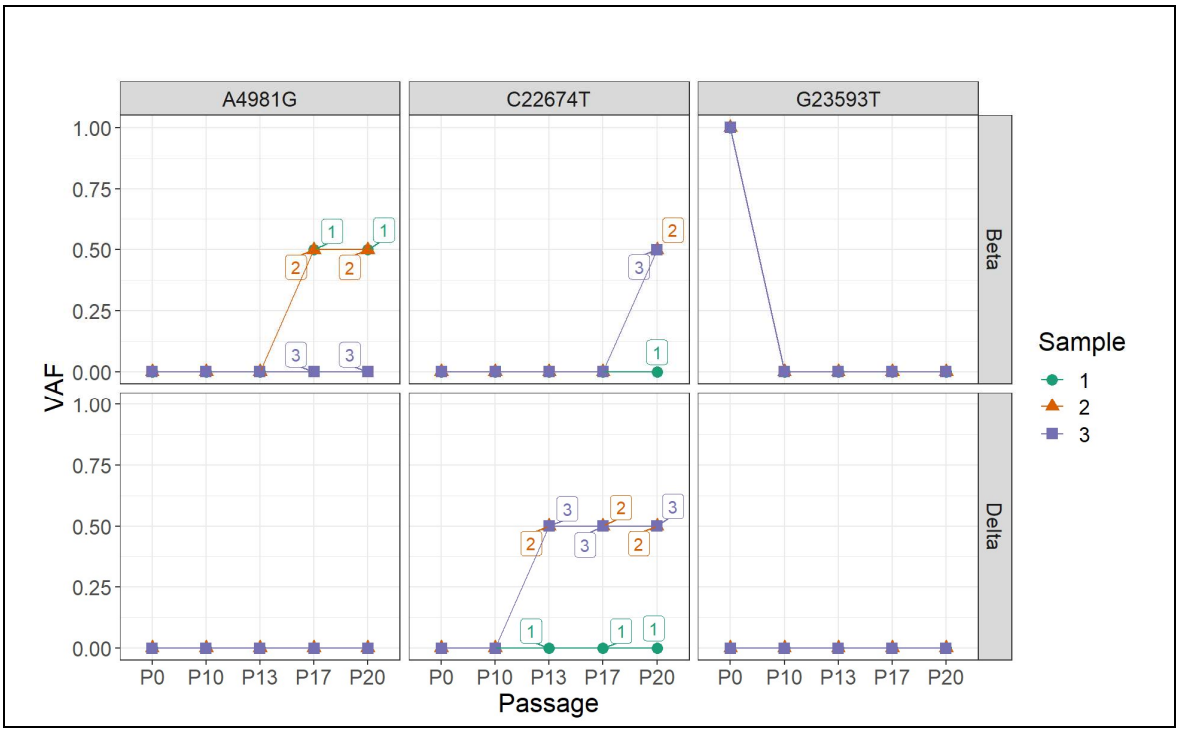

364 **Figure 4. Variants of clinical relevance arose de novo and grew to dominance**. VAF:

365 variant allele frequency. P refers to passage.

366 **Table 1. Annotations of select variants that changed in frequency across the study.**

Variant	Amino Acid Change	Annotation
A4981G	ORF1ab T1572T	Mutations that may confer drug resistance[20]
C22674T	Spike S371F	Protein interacting, antibody escape, vaccine target, Omicron-associated variant allele[20]
G23593T	Spike Q677H	Protein interacting, vaccine target[20], enhances treatment resistance[31], increases infectivity[31]

367

368

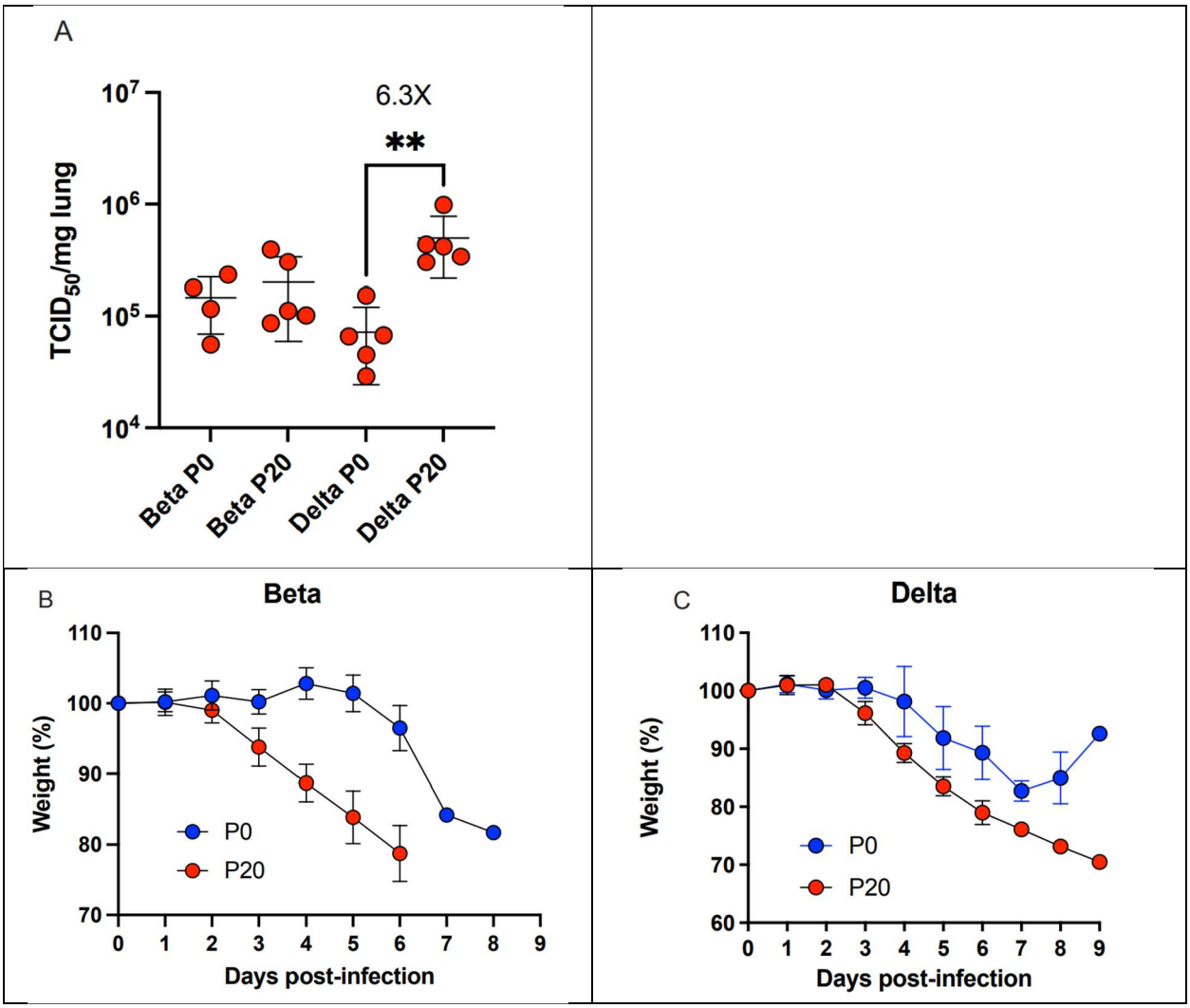

369 **Figure 5. Pathogenesis of P0 and P20 viruses in K18-ACE2 mice**. Mice (n = 15/group) were

370 infected with 500 $TCID_{50}$ of P0 or P20 Beta and Delta viruses. (A) On day 3 post-infection, mice

371 (n = 5) were euthanized and lungs collected for infectious viral load determination. Results are

372 expressed as mean ± SD SARS-CoV-2 $TCID_{50}$/mg of lung tissue. (B-C) The weight of each

373 mouse (n = 10/group) was monitored daily throughout the experiment and reported as mean

374 percentage ± SD of weight relative to day 0. **: $p \leq 0.008$ as determined using non-parametric

375 Mann-Whitney test.

376

377

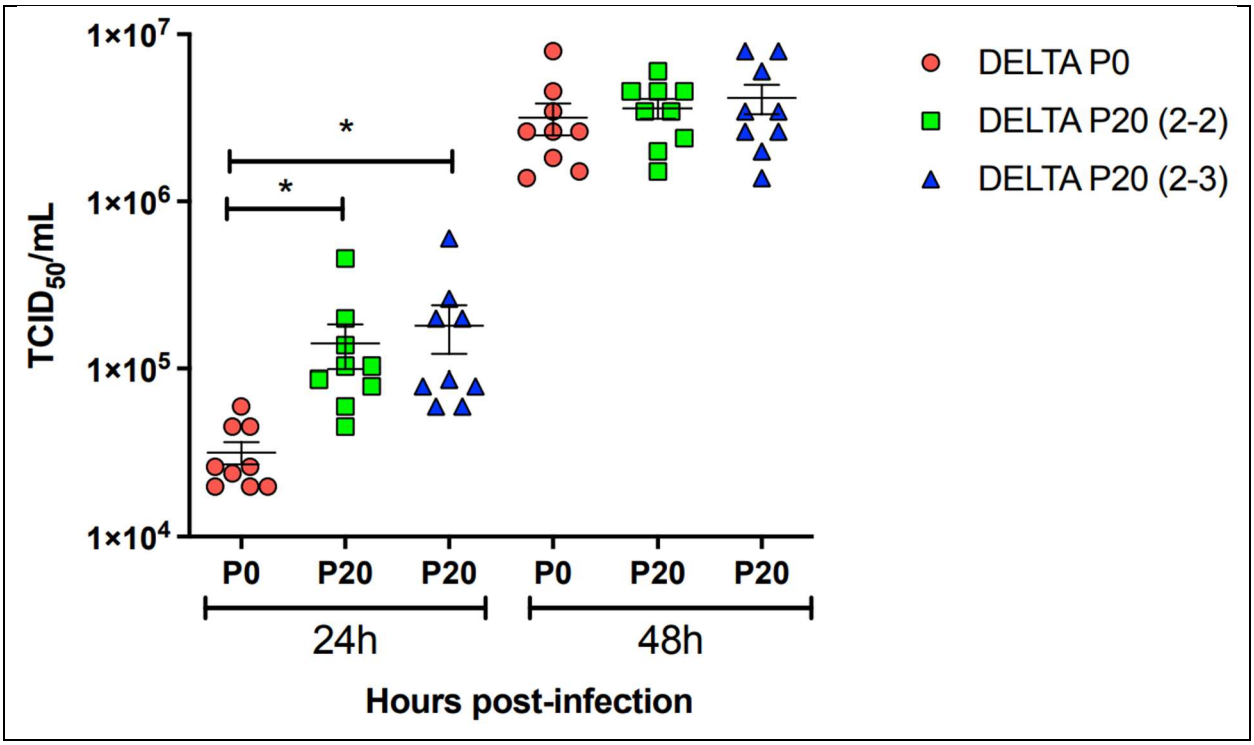

378 **Figure 6**. **Growth kinetics of P0 and P20 Delta viruses**. P0 and two independently evolved

379 P20 Delta viruses were used to infect Vero cells at a multiplicity of infection of 0.005. Cell-free

380 supernatants were collected at 24 h and 48 h and used for viral titration. Results are expressed

381 as mean ± SD $TCID_{50}$/mL. *: p=0.02 as determined using an unpaired t-test.

382

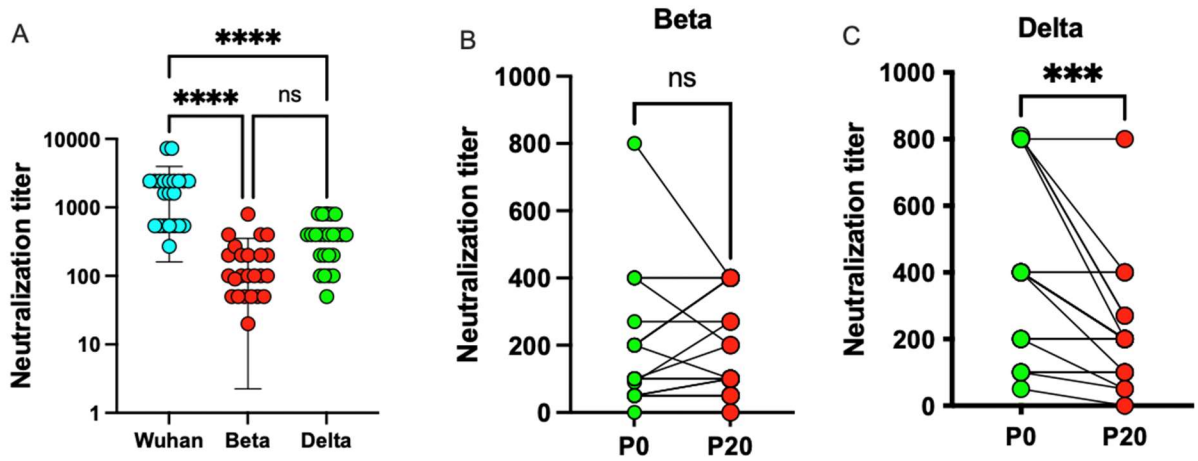

Figure 7. Neutralization of P0 and P20 viruses with sera from vaccinated subjects. (A) Neutralization assay of Wuhan-like, Beta, and Delta viruses using sera from 24 vaccinated subjects. Individual results and mean ± SD neutralization titer against different SARS-CoV-2 isolates are presented. ****: $p<0.0001$ determined using one way-ANOVA. ns: not statistically significant. (B) Pair-wise comparison of the sera used in A in neutralization assay against P0 and P20 Beta viruses. (C) Pair-wise comparison of the sera used in A in neutralization assay against P0 and P20 Delta viruses. ***: $p>0.002$ determined using paired t-test.

391 **Supplemental Figures**

392 **Supplemental Table 1. Table of variant alleles that changed MAF during the study.**

393 **Available in "Supplemental Tables.csv".**

394

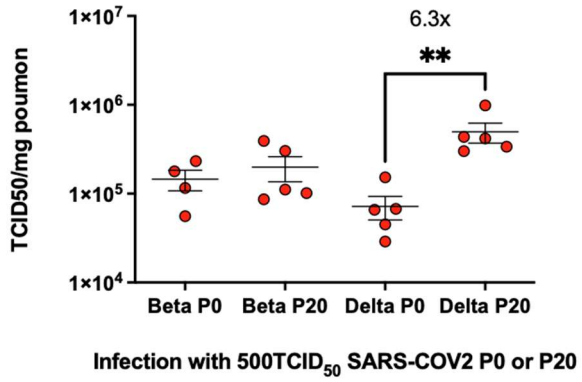

395

396 **Supplemental Figure 1. Viral load comparison between P0 and P20 virus in K18-ACE2**

397 **mice.**

398

399

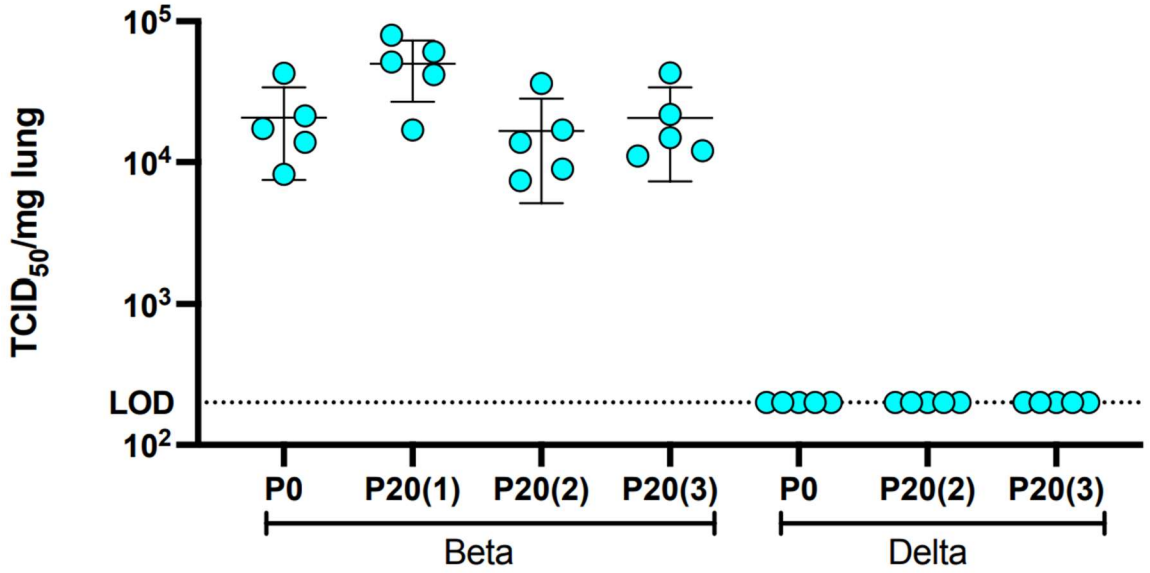

400

401 **Supplementary Figure 2. Infection of C57BL6 mice with P0 and P20 Beta and Delta**

402 **viruses**. Mice (n = 5/group) were infected intranasally with 3000 $TCID_{50}$ of P0 or three

403 independently evolved Beta P20 or two independently evolved Delta viruses. On the third day

404 post infection, mice were euthanized and lungs collected for infectious viral load determination.

405 Individual results and mean ± SD $TCID_{50}$/mg of lung tissue are presented.

406

407 **References**:

408 1. Jacobs, J.L., Haidar, G. & Mellors, J.W. COVID-19: Challenges of Viral Variants. *Annu*

409 *Rev Med* (2022).

410 2. Sun, F. *et al.* SARS-CoV-2 Quasispecies Provides an Advantage Mutation Pool for the

411 Epidemic Variants. *Microbiol Spectr* **9**, e0026121 (2021).

412 3. Velavan, T.P. *et al.* Host genetic factors determining COVID-19 susceptibility and

413 severity. *EBioMedicine* **72**, 103629 (2021).

414 4. Belsky, J.A. *et al.* COVID-19 in immunocompromised patients: A systematic review of
415 cancer, hematopoietic cell and solid organ transplant patients. *J Infect* **82**, 329-338
416 (2021).
417 5. Van Cleemput, J. *et al.* Organ-specific genome diversity of replication-competent SARS-
418 CoV-2. *Nat Commun* **12**, 6612 (2021).
419 6. Wang, R., Chen, J. & Wei, G.W. Mechanisms of SARS-CoV-2 Evolution Revealing
420 Vaccine-Resistant Mutations in Europe and America. *J Phys Chem Lett* **12**, 11850-
421 11857 (2021).
422 7. Liu, Y. *et al.* The N501Y spike substitution enhances SARS-CoV-2 infection and
423 transmission. *Nature* **602**, 294-299 (2022).
424 8. Motozono, C. *et al.* SARS-CoV-2 spike L452R variant evades cellular immunity and
425 increases infectivity. *Cell Host Microbe* **29**, 1124-1136 e11 (2021).
426 9. Cherian, S. *et al.* SARS-CoV-2 Spike Mutations, L452R, T478K, E484Q and P681R, in
427 the Second Wave of COVID-19 in Maharashtra, India. *Microorganisms* **9**(2021).
428 10. Liu, Y. *et al.* Delta spike P681R mutation enhances SARS-CoV-2 fitness over Alpha
429 variant. *Cell Rep* **39**, 110829 (2022).
430 11. Planas, D. *et al.* Reduced sensitivity of SARS-CoV-2 variant Delta to antibody
431 neutralization. *Nature* **596**, 276-280 (2021).
432 12. Gu, H. *et al.* Adaptation of SARS-CoV-2 in BALB/c mice for testing vaccine efficacy.
433 *Science* **369**, 1603-1607 (2020).
434 13. Wasik, B.R. *et al.* Influenza Viruses in Mice: Deep Sequencing Analysis of Serial
435 Passage and Effects of Sialic Acid Structural Variation. *J Virol* **93**(2019).
436 14. Sun, S. *et al.* Characterization and structural basis of a lethal mouse-adapted SARS-
437 CoV-2. *Nat Commun* **12**, 5654 (2021).
438 15. Huang, K. *et al.* Q493K and Q498H substitutions in Spike promote adaptation of SARS-
439 CoV-2 in mice. *EBioMedicine* **67**, 103381 (2021).

440 16. Chung, H., Noh, J.Y., Koo, B.S., Hong, J.J. & Kim, H.K. SARS-CoV-2 mutations
441 acquired during serial passage in human cell lines are consistent with several of those
442 found in recent natural SARS-CoV-2 variants. *Comput Struct Biotechnol J* **20**, 1925-
443 1934 (2022).
444 17. Sonnleitner, S.T. *et al.* The mutational dynamics of the SARS-CoV-2 virus in serial
445 passages in vitro. *Virol Sin* **37**, 198-207 (2022).
446 18. Tonkin-Hill, G. *et al.* Patterns of within-host genetic diversity in SARS-CoV-2. *Elife*
447 **10**(2021).
448 19. Turakhia, Y. *et al.* Pandemic-scale phylogenomics reveals the SARS-CoV-2
449 recombination landscape. *Nature* **609**, 994-997 (2022).
450 20. Kent, W.J. *et al.* The human genome browser at UCSC. *Genome Res* **12**, 996-1006
451 (2002).
452 21. Cao, Y. *et al.* BA.2.12.1, BA.4 and BA.5 escape antibodies elicited by Omicron infection.
453 *Nature* **608**, 593-602 (2022).
454 22. Johnson, B.A. *et al.* Loss of furin cleavage site attenuates SARS-CoV-2 pathogenesis.
455 *Nature* **591**, 293-299 (2021).
456 23. Tada, T. *et al.* Convalescent-Phase Sera and Vaccine-Elicited Antibodies Largely
457 Maintain Neutralizing Titer against Global SARS-CoV-2 Variant Spikes. *mBio* **12**,
458 e0069621 (2021).
459 24. Dupont, L. *et al.* Neutralizing antibody activity in convalescent sera from infection in
460 humans with SARS-CoV-2 and variants of concern. *Nat Microbiol* **6**, 1433-1442 (2021).
461 25. Tarres-Freixas, F. *et al.* Heterogeneous Infectivity and Pathogenesis of SARS-CoV-2
462 Variants Beta, Delta and Omicron in Transgenic K18-hACE2 and Wildtype Mice. *Front*
463 *Microbiol* **13**, 840757 (2022).
464 26. Rahimi, F. & Talebi Bezmin Abadi, A. Implications of the Emergence of a New Variant of
465 SARS-CoV-2, VUI-202012/01. *Arch Med Res* **52**, 569-571 (2021).

466 27. Sedova, M., Jaroszewski, L., Iyer, M. & Godzik, A. Monitoring for SARS-CoV-2 drug
467 resistance mutations in broad viral populations. *bioRxiv* (2022).
468 28. Kandeel, M. *et al.* Repurposing of FDA-approved antivirals, antibiotics, anthelmintics,
469 antioxidants, and cell protectives against SARS-CoV-2 papain-like protease. *J Biomol*
470 *Struct Dyn* **39**, 5129-5136 (2021).
471 29. Hammond, J. *et al.* Oral Nirmatrelvir for High-Risk, Nonhospitalized Adults with Covid-
472 19. *N Engl J Med* **386**, 1397-1408 (2022).
473 30. Pastorio, C. *et al.* Determinants of Spike infectivity, processing, and neutralization in
474 SARS-CoV-2 Omicron subvariants BA.1 and BA.2. *Cell Host Microbe* **30**, 1255-1268 e5
475 (2022).
476 31. Zeng, C. *et al.* Neutralization of SARS-CoV-2 Variants of Concern Harboring Q677H.
477 *mBio* **12**, e0251021 (2021).
478 32. Kim, K. *et al.* The roles of APOBEC-mediated RNA editing in SARS-CoV-2 mutations,
479 replication and fitness. *Sci Rep* **12**, 14972 (2022).
480 33. Lei, C., Yang, J., Hu, J. & Sun, X. On the Calculation of TCID(50) for Quantitation of
481 Virus Infectivity. *Virol Sin* **36**, 141-144 (2021).
482 34. Garrison, E.P.M.G. Haplotype-based variant detection from short-read sequencing. *arXiv*
483 (2012).
484 35. N'Guessan A, T.A., Sanchez-Quete F, Goitom E, Reiling SJ, Galvez JH, Nguyen TL,
485 Nguyen HTL, Visentin F, Hachad M, Krylova K, Matthews S, Kraemer SA, Stretenowich
486 P, Bourgey M, Djambazian H, Chen S, Roy A, Brookes B, Lee S, Simon M, Maere T,
487 Vanrolleghem PA, Labelle M, Moreira S, Levade I, Bourque G, Ragoussis J, Dorner S,
488 Frigon D, Shapiro BJ. Detection of prevalent SARS-CoV-2 variant lineages in
489 wastewater and clinical sequences from cities in Québec, Canada. *medRxiv* (2022).
490 36. Gerstung, M. *et al.* Reliable detection of subclonal single-nucleotide variants in tumour
491 cell populations. *Nat Commun* **3**, 811 (2012).

492 37. Rao, R.S.P. *et al.* Evolutionary Dynamics of Indels in SARS-CoV-2 Spike Glycoprotein.
493 *Evol Bioinform Online* **17**, 11769343211064616 (2021).
494 38. Ramachandran, V.K. *et al.* Comparison of variant callers for wastewater-based
495 epidemiology. *medRxiv* (2022).
496 39. Li, H. Aligning sequence reads, clone sequences and assembly contigs with BWA-MEM.
497 *arXiv* (2013).
498 40. McLaren, W. *et al.* The Ensembl Variant Effect Predictor. *Genome Biol* **17**, 122 (2016).

499